

Electronic supplementary information

**The smallest endohedral borafullerene: structural isomerization,
electronic property, aromaticity and reactivity of U@C₂₇B**

Xinde Li, Lei Lou and Peng Jin*

School of Materials Science and Engineering, Hebei University of Technology,

Tianjin 300130, China. E-mail: china.peng.jin@gmail.com

Table S1 Relative energies (ΔE , kcal/mol) of ten C₂₇B isomers with different spin multiplicities (M) at the PBE0/6-311G*~SDD level of theory.

Isomers	M	ΔE
<i>T_d</i> -C ₂₇ B-1	2	26.2
	4	19.8
	6	19.0
<i>T_d</i> -C ₂₇ B-2	2	11.5
	4	3.8
	6	35.0
<i>T_d</i> -C ₂₇ B-3	2	8.6
	4	0.0
	6	21.2
<i>D₂</i> -C ₂₇ B-1	2	30.6
	4	39.9
	6	61.9
<i>D₂</i> -C ₂₇ B-2	2	41.5
	4	47.1
	6	69.1
<i>D₂</i> -C ₂₇ B-3	2	23.8
	4	39.6
	6	60.8
<i>D₂</i> -C ₂₇ B-4	2	38.6
	4	42.7
	6	63.8
<i>D₂</i> -C ₂₇ B-5	2	40.6
	4	48.1
	6	70.5
<i>D₂</i> -C ₂₇ B-6	2	41.9
	4	51.8
	6	74.8

	2	48.2
$D_2\text{-C}_{27}\text{B}^6\text{-7}$	4	49.2
	6	70.8

Table S2 Relative energies (ΔE , kcal/mol) of ten $\text{C}_{27}\text{B}^{6-}$ isomers with different spin multiplicities (M) at PBE0/6-311G*~SDD level of theory.

Isomers	M	ΔE
	2	0.0
$T_d\text{-C}_{27}\text{B}^{6-}\text{-1}$	4	40.2
	2	7.8
$T_d\text{-C}_{27}\text{B}^{6-}\text{-2}$	4	40.7
	2	0.6
$T_d\text{-C}_{27}\text{B}^{6-}\text{-3}$	4	34.2
	2	29.1
$D_2\text{-C}_{27}\text{B}^{6-}\text{-1}$	4	49.8
	2	40.1
$D_2\text{-C}_{27}\text{B}^{6-}\text{-2}$	4	58.6
	2	35.8
$D_2\text{-C}_{27}\text{B}^{6-}\text{-3}$	4	56.2
	2	37.6
$D_2\text{-C}_{27}\text{B}^{6-}\text{-4}$	4	57.1
	2	40.6
$D_2\text{-C}_{27}\text{B}^{6-}\text{-5}$	4	61.2
	2	47.7
$D_2\text{-C}_{27}\text{B}^{6-}\text{-6}$	4	66.4
	2	44.6
$D_2\text{-C}_{27}\text{B}^{6-}\text{-7}$	4	62.4

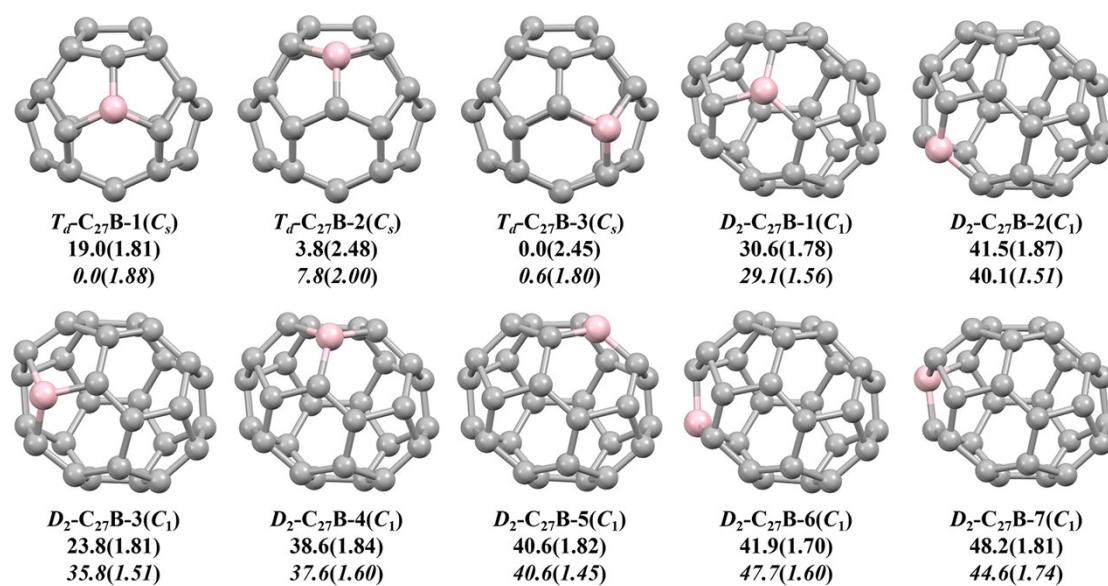


Fig. S1 Optimized structures and molecular symmetries of ten C_{27}B isomers with relative energies (kcal/mol) and SOMO-LUMO gap energies (eV, in parentheses). The results for their hexaanions are also given in italic fonts (whose structures are omitted because they are very similar to the neutral ones). B: pink; C: gray.

Table S3 Relative energies (kcal/mol) of ten $\text{U}@C_{27}\text{B}$ isomers with different spin multiplicities (M) at different levels of theory.

Isomers	M	PBE0	B3LYP	M06-2X
$\text{U}@T_d\text{-C}_{27}\text{B-1}$	2	0.0	0.0	0.0
	4	67.0	64.3	71.5
$\text{U}@T_d\text{-C}_{27}\text{B-2}$	2	13.2	13.0	14.4
	4	59.5	57.8	63.8
$\text{U}@T_d\text{-C}_{27}\text{B-3}$	2	0.1	0.1	0.5
	4	55.1	53.2	60.0
$\text{U}@D_2\text{-C}_{27}\text{B-1}$	2	75.6	71.9	75.6
	4	110.5	105.7	111.9
$\text{U}@D_2\text{-C}_{27}\text{B-2}$	2	92.1	88.0	92.2
	4	128.3	123.0	130.0
$\text{U}@D_2\text{-C}_{27}\text{B-3}$	2	87.5	83.6	88.0
	4	122.2	117.1	124.1
$\text{U}@D_2\text{-C}_{27}\text{B-4}$	2	90.7	86.7	91.1
	4	127.0	121.5	123.3
$\text{U}@D_2\text{-C}_{27}\text{B-5}$	2	93.8	89.7	94.0

	4	130.7	125.3	131.8
U@D ₂ -C ₂₇ B ⁻⁶	2	103.9	99.7	104.6
	4	139.7	134.3	142.6
U@D ₂ -C ₂₇ B ⁻⁷	2	105.6	101.2	106.2
	4	144.5	137.9	147.6

Table S4 Relative energies (kcal/mol) of ten U@C₂₇B⁺ cation isomers with different spin multiplicities (*M*) at different levels of theory.

Isomers	<i>M</i>	PBE0	B3LYP	M06-2X
U@T _d -C ₂₇ B ⁺¹	1	0.5	0.5	0.0
	3	63.0	60.5	67.0
U@T _d -C ₂₇ B ⁺²	1	13.4	14.0	14.0
	3	60.1	58.0	63.2
U@T _d -C ₂₇ B ⁺³	1	0.0	0.0	0.1
	3	55.0	52.8	58.7
U@D ₂ -C ₂₇ B ⁺¹	1	95.2	90.5	96.3
	3	114.8	109.3	118.3
U@D ₂ -C ₂₇ B ⁺²	1	105.8	101.0	106.6
	3	134.0	128.0	137.6
U@D ₂ -C ₂₇ B ⁺³	1	105.3	100.4	107.0
	3	125.7	120.1	129.1
U@D ₂ -C ₂₇ B ⁺⁴	1	108.3	103.3	109.8
	3	125.1	119.7	128.1
U@D ₂ -C ₂₇ B ⁺⁵	1	106.3	101.5	107.2
	3	135.4	129.4	139.0
U@D ₂ -C ₂₇ B ⁺⁶	1	116.2	111.2	117.7
	3	145.6	139.4	149.9
U@D ₂ -C ₂₇ B ⁺⁷	1	117.9	113.0	119.6
	3	144.5	138.7	148.4

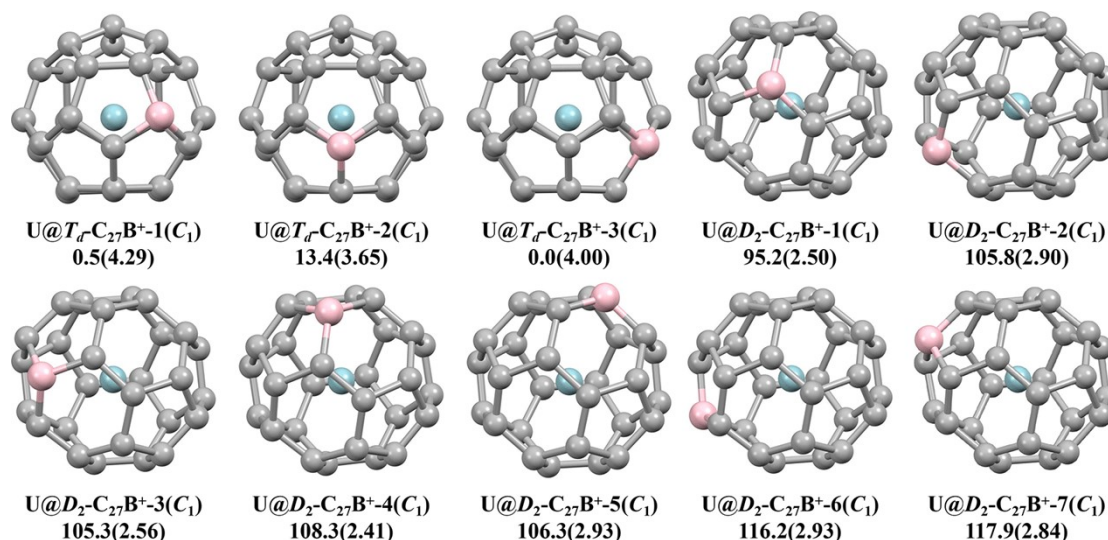


Fig. S2 Optimized structures and molecular symmetries of ten $U@C_{27}B^+$ cation isomers with relative energies (kcal/mol) and HOMO-LUMO gap energies (eV, in parentheses). U: blue; B: pink; C: gray.

Table S5 Relative energies (ΔE , kcal/mol) and $\Sigma\theta_p$ (in degree) of two C_{28} isomers and ten $C_{27}B$, $C_{27}B^{6-}$, $U@C_{27}B$, $U@C_{27}B^+$ isomers.

Isomers	ΔE	$\Sigma\theta_p$	Isomers	ΔE	$\Sigma\theta_p$
T_d-C_{28}	0.0	486.57	$D_2-C_{27}B^{6-}-7$	44.6	493.71
D_2-C_{28}	33.6	491.87	$U@T_d-C_{27}B-1$	0.0	486.33
$T_d-C_{27}B-1$	19.0	486.84	$U@T_d-C_{27}B-2$	13.2	486.71
$T_d-C_{27}B-2$	3.8	486.46	$U@T_d-C_{27}B-3$	0.1	486.04
$T_d-C_{27}B-3$	0.0	486.13	$U@D_2-C_{27}B-1$	75.6	490.67
$D_2-C_{27}B-1$	30.6	491.50	$U@D_2-C_{27}B-2$	92.1	491.49
$D_2-C_{27}B-2$	41.5	492.34	$U@D_2-C_{27}B-3$	87.5	491.22
$D_2-C_{27}B-3$	23.8	491.47	$U@D_2-C_{27}B-4$	90.7	491.46
$D_2-C_{27}B-4$	38.6	492.43	$U@D_2-C_{27}B-5$	93.8	491.30
$D_2-C_{27}B-5$	40.6	492.38	$U@D_2-C_{27}B-6$	103.9	492.10
$D_2-C_{27}B-6$	41.9	492.62	$U@D_2-C_{27}B-7$	105.6	492.18
$D_2-C_{27}B-7$	48.2	492.53	$U@T_d-C_{27}B^+-1$	0.5	486.67
$T_d-C_{27}B^{6-}-1$	0.0	487.98	$U@T_d-C_{27}B^+-2$	13.4	487.07
$T_d-C_{27}B^{6-}-2$	7.8	488.28	$U@T_d-C_{27}B^+-3$	0.0	486.43
$T_d-C_{27}B^{6-}-3$	0.6	487.41	$U@D_2-C_{27}B^+-1$	95.2	490.25
$D_2-C_{27}B^{6-}-1$	29.1	492.79	$U@D_2-C_{27}B^+-2$	105.8	491.17

$D_2-C_{27}B^{6-}2$	40.1	493.55	$U@D_2-C_{27}B^{+}3$	105.3	490.90
$D_2-C_{27}B^{6-}3$	35.8	492.97	$U@D_2-C_{27}B^{+}4$	108.3	491.05
$D_2-C_{27}B^{6-}4$	37.6	493.75	$U@D_2-C_{27}B^{+}5$	106.3	490.92
$D_2-C_{27}B^{6-}5$	40.6	493.57	$U@D_2-C_{27}B^{+}6$	116.2	491.76
$D_2-C_{27}B^{6-}6$	47.7	493.99	$U@D_2-C_{27}B^{+}7$	117.9	491.92

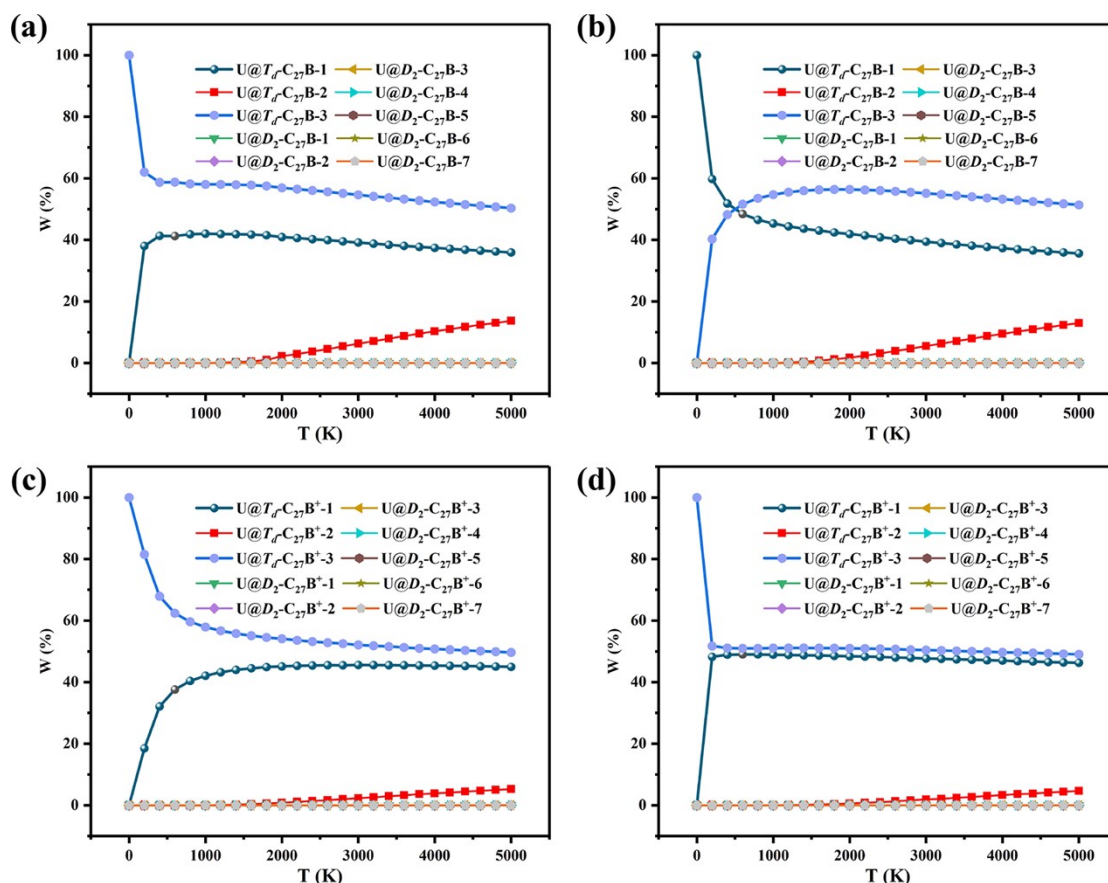


Fig. S3 Relative concentrations of the ten $U@C_{27}B^{0+}$ isomers at the (a)(c) B3LYP and (b)(d) M06-2X levels of theory.

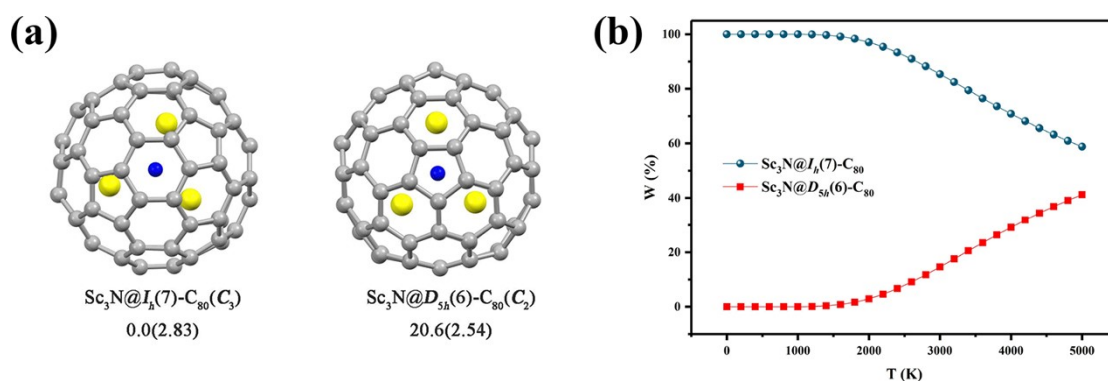


Fig. S4 (a) Optimized structures and molecular symmetries of two $\text{Sc}_3\text{N}@C_{80}$ isomers with relative energies (kcal/mol) and HOMO-LUMO gap energies (eV, in parentheses) as well as (b) Their relative concentrations at different temperatures at the PBE0/6-311G*~SDD level of theory. C: gray; N: blue; Sc: yellow.

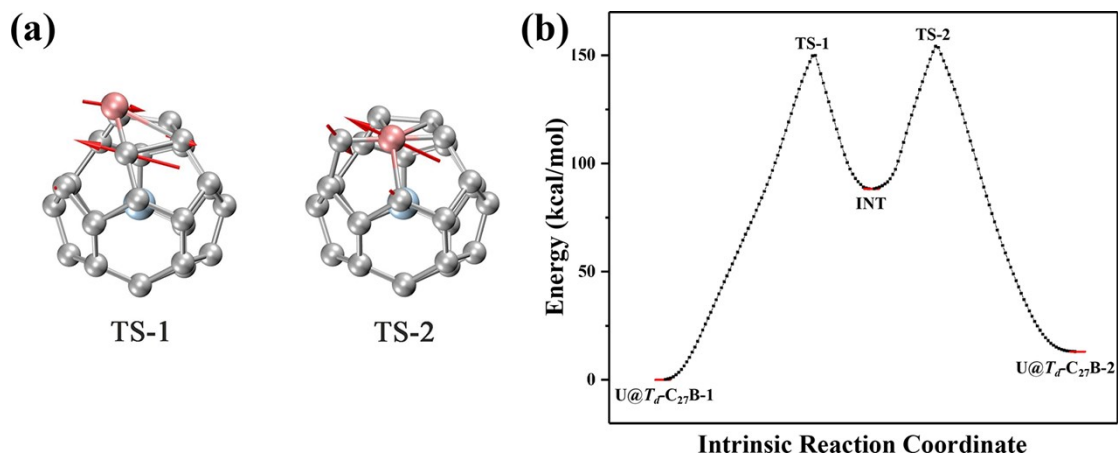


Fig. S5 (a) Vibrational mode of the only imaginary frequency for TS-1 and TS-2; (b) Intrinsic reaction coordinate from $\text{U}@T_d\text{-C}_{27}\text{B-1}$ to $\text{U}@T_d\text{-C}_{27}\text{B-2}$.

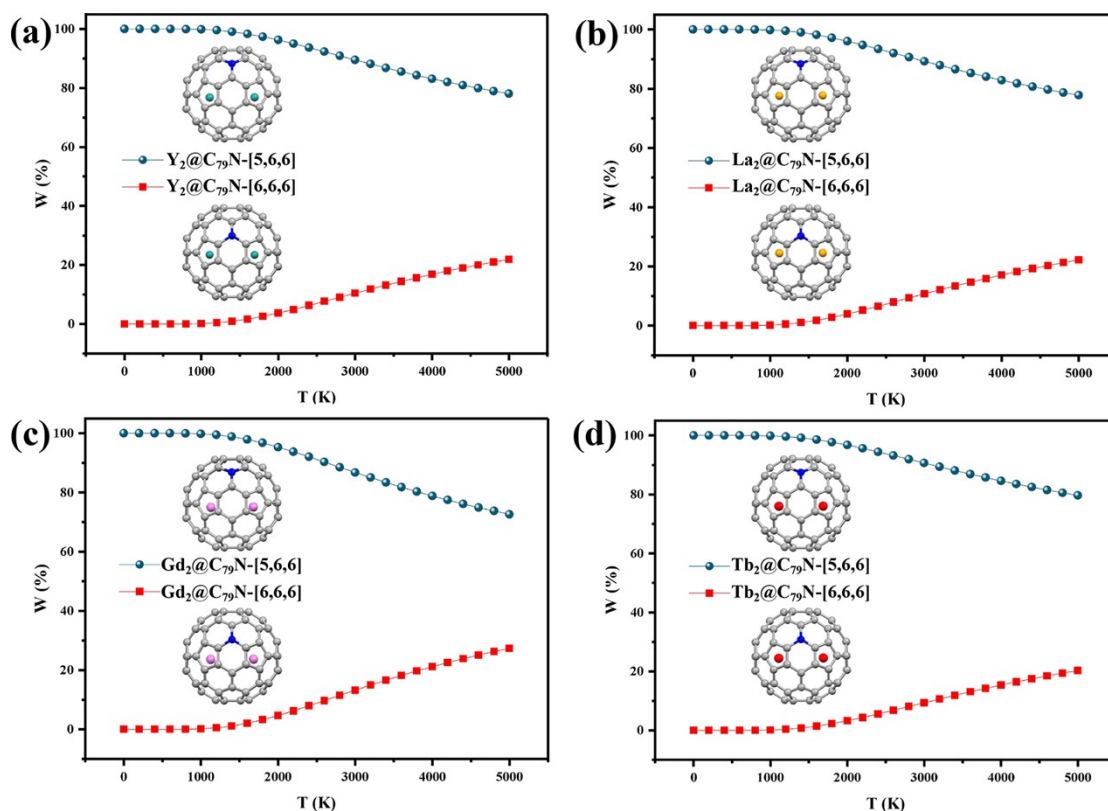


Fig. S6 Relative concentrations of two (a) $\text{Y}_2@C_{79}\text{N}$, (b) $\text{La}_2@C_{79}\text{N}$, (c) $\text{Gd}_2@C_{79}\text{N}$ and (d) $\text{Tb}_2@C_{79}\text{N}$ azafullerene isomers at different temperatures at the PBE0/6-

311G*~SDD level of theory.

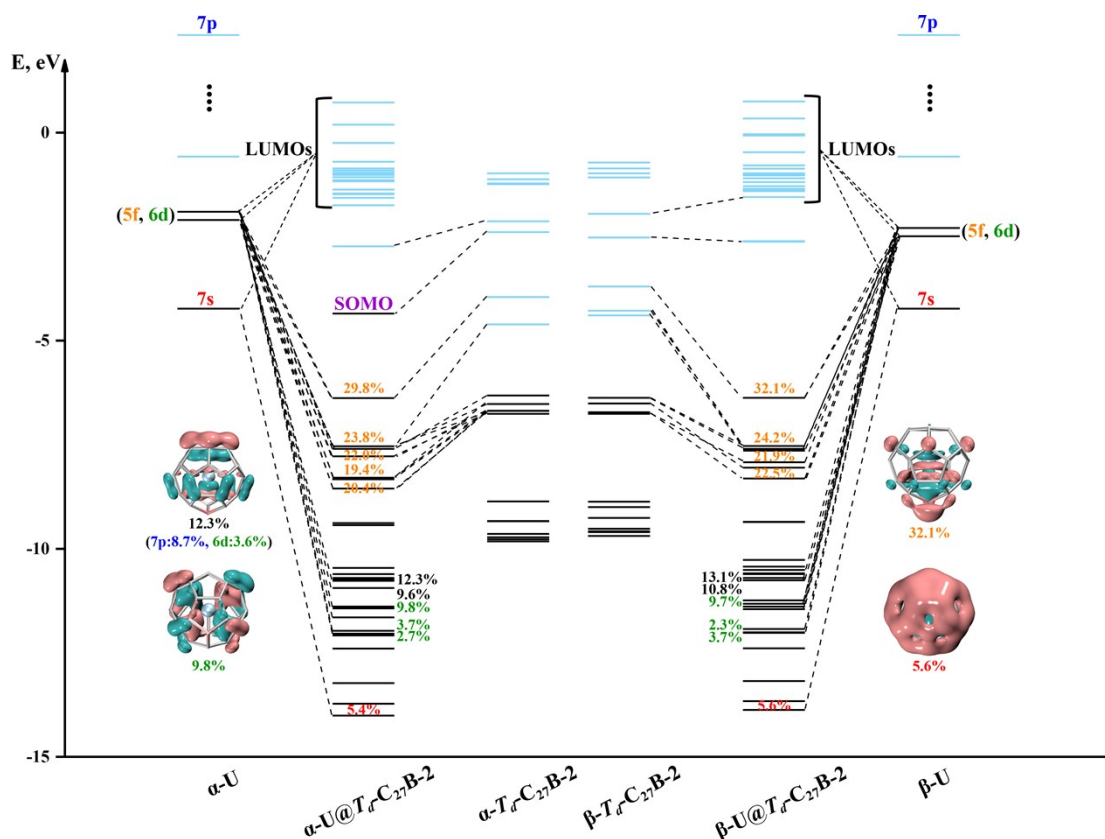


Fig. S7 Orbital interaction diagram of $U@T_d-C_{27}B-2$. Occupied and unoccupied orbitals are denoted by black and blue lines, respectively. Total metal contributions to the occupied hybrid orbitals are given in %. Selected occupied orbitals with maximum contributions from each type of metal valence orbitals (isovalue: ± 0.05 a.u.) are plotted.

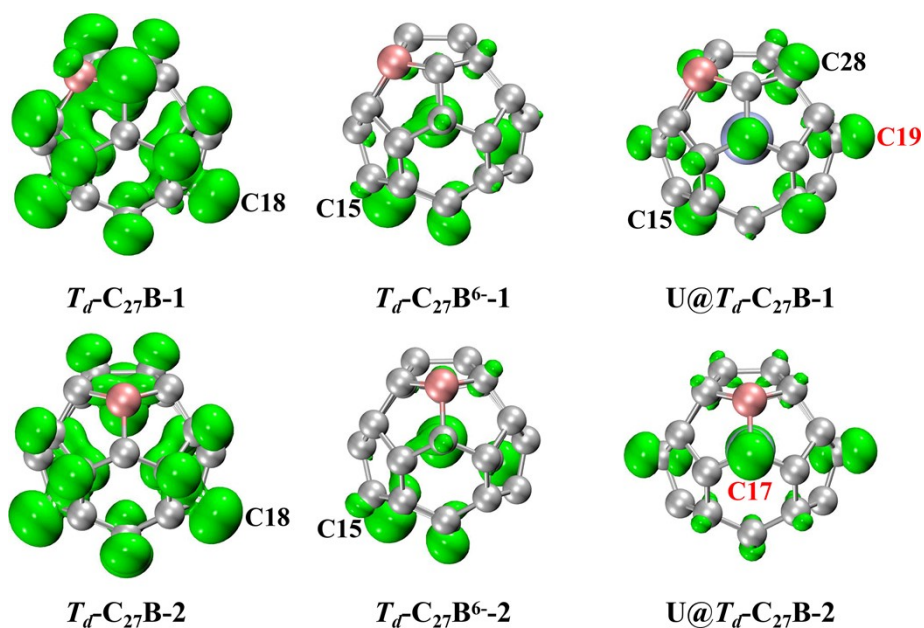


Fig. S8 Spin density distributions (isovalue: ± 0.005 a.u.) of two T_d - $C_{27}B$, T_d - $C_{27}B^{6-}$ and $U@T_d$ - $C_{27}B$ isomers. The carbon sites with large spin densities are shown. The sites for trifluoromethylation are highlighted in red.

Table S6 AIM charges for the U atom, B atom and its C neighbors (average value) of T_d - $C_{27}B^{0/6-}$ and $U@T_d$ - $C_{27}B^{0/+}$ isomers (PBE0/6-311G*~SDD level).

Isomers	Atom	Charge
T_d - $C_{27}B$ -1	B	+1.85
	C	-0.59
T_d - $C_{27}B$ -2	B	+1.89
	C	-0.62
T_d - $C_{27}B^{6-}$ -1	B	+1.69
	C	-0.93
T_d - $C_{27}B^{6-}$ -2	B	+1.06
	C	-0.68
$U@T_d$ - $C_{27}B$ -1	U	+2.04
	B	+1.77
	C	-0.65
$U@T_d$ - $C_{27}B$ -2	U	+2.04
	B	+1.73
	C	-0.65
$U@T_d$ - $C_{27}B^{+}$ -1	U	+2.01
	B	+1.81
	C	-0.61
$U@T_d$ - $C_{27}B^{+}$ -2	U	+1.99
	B	+1.76
	C	-0.60

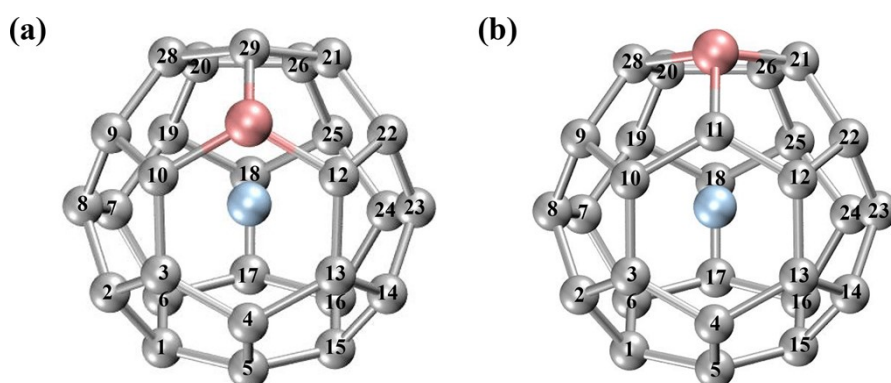
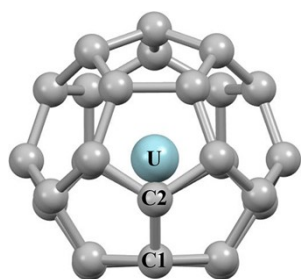


Fig. S9 Molecular structures of (a) $U@T_d-C_{27}B-1$ and (b) $U@T_d-C_{27}B-2$ with atom numbering for studying U-cage interactions.

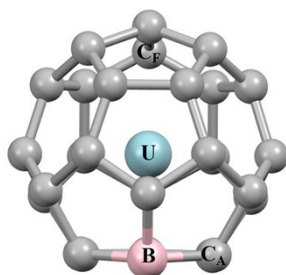
Table S7 Bond lengths (d , Å), Wiberg bond indices (WBIs), Mayer bond orders (MBOs), delocalization indices (δ) and their respective sum for the U-cage interactions in $U@T_d-C_{27}B$. See Fig. S9 for the atom numbering.

Isomer	Atom pairs	d	WBI	MBO	δ	Isomer	Atom pairs	d	WBI	MBO	δ
$U@T_d-C_{27}B-1$	U-C1	2.47	0.52	0.30	0.26	$U@T_d-C_{27}B-2$	U-C1	2.45	0.53	0.29	0.27
	U-C2	2.48	0.55	0.37	0.30		U-C2	2.49	0.55	0.38	0.30
	U-C3	2.45	0.53	0.30	0.27		U-C3	2.43	0.54	0.29	0.27
	U-C4	2.41	0.61	0.36	0.33		U-C4	2.43	0.58	0.34	0.30
	U-C5	2.42	0.59	0.34	0.31		U-C5	2.45	0.57	0.34	0.30
	U-C6	2.44	0.57	0.34	0.30		U-C6	2.44	0.56	0.34	0.30
	U-C7	2.44	0.58	0.34	0.31		U-C7	2.43	0.58	0.33	0.30
	U-C8	2.43	0.56	0.30	0.28		U-C8	2.47	0.51	0.29	0.25
	U-C9	2.43	0.59	0.36	0.32		U-C9	2.42	0.59	0.36	0.32
	U-C10	2.48	0.57	0.40	0.35		U-C10	2.42	0.59	0.36	0.32
	U-B	2.57	0.48	0.26	0.09		U-C11	2.54	0.50	0.35	0.30
	U-C12	2.48	0.57	0.40	0.35		U-C12	2.42	0.59	0.36	0.32
	U-C13	2.45	0.53	0.30	0.27		U-C13	2.44	0.54	0.29	0.27

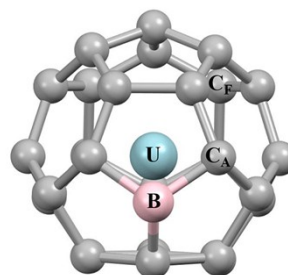
U-C14	2.48	0.55	0.37	0.30	U-C14	2.49	0.55	0.38	0.30	
U-C15	2.47	0.52	0.30	0.26	U-C15	2.45	0.53	0.29	0.27	
U-C16	2.44	0.57	0.34	0.30	U-C16	2.44	0.56	0.34	0.30	
U-C17	2.45	0.55	0.32	0.28	U-C17	2.52	0.47	0.27	0.22	
U-C18	2.50	0.53	0.37	0.29	U-C18	2.50	0.54	0.38	0.29	
U-C19	2.48	0.51	0.29	0.25	U-C19	2.44	0.54	0.29	0.27	
U-C20	2.42	0.58	0.34	0.31	U-C20	2.42	0.60	0.36	0.32	
U-C21	2.47	0.52	0.30	0.26	U-C21	2.49	0.53	0.34	0.32	
U-C22	2.43	0.59	0.36	0.32	U-C22	2.42	0.59	0.36	0.32	
U-C23	2.43	0.56	0.30	0.28	U-C23	2.48	0.51	0.29	0.25	
U-C24	2.44	0.58	0.34	0.31	U-C24	2.43	0.58	0.33	0.30	
U-C25	2.48	0.51	0.29	0.25	U-C25	2.44	0.54	0.29	0.27	
U-C26	2.42	0.59	0.35	0.31	U-C26	2.42	0.60	0.36	0.32	
U-C28	2.47	0.52	0.30	0.26	U-C28	2.49	0.53	0.34	0.32	
U-C29	2.55	0.52	0.42	0.33	U-B	2.62	0.51	0.34	0.12	
Sum	-	68.88	15.45	9.36	8.05	-	68.88	15.41	9.28	8.01



$U@T_d-C_{28}$



$U@T_d-C_{27}B-1$



$U@T_d-C_{27}B-2$

Fig. S10 Structures of $U@T_d-C_{28}$, $U@T_d-C_{27}B-1$ and $U@T_d-C_{27}B-2$ with corresponding U, B, C sites used in the IQA analyses.

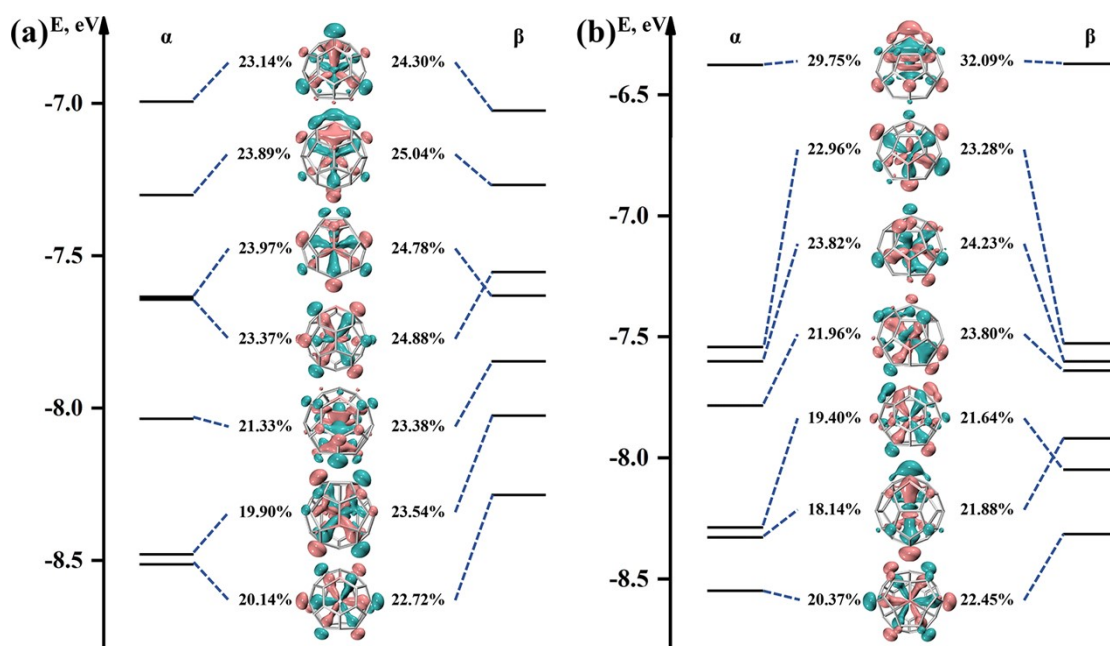


Fig. S11 Some occupied molecular orbitals of (a) $U@T_d-C_{27}B-1$ and (b) $U@T_d-C_{27}B-2$ (isovalue: ± 0.05 a.u.) with total contribution (%) of U-5f to the orbital.

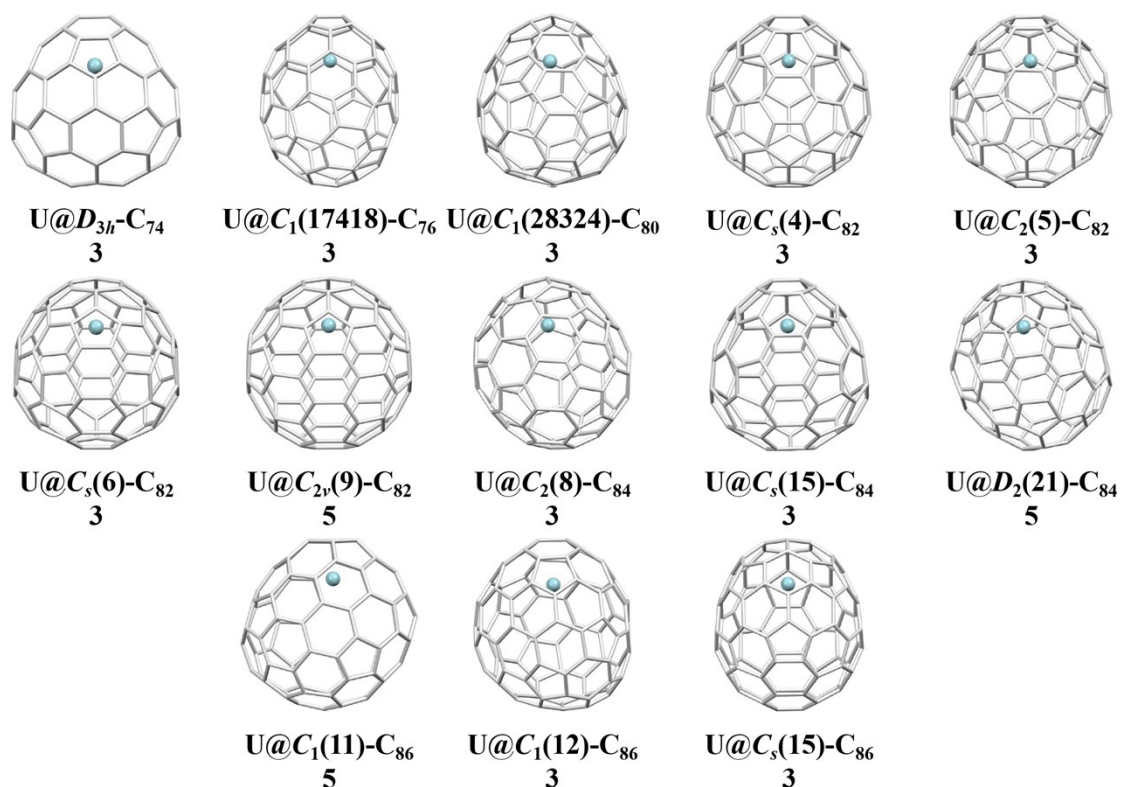


Fig. S12 Optimized ground-state structures with spin multiplicities of all 13 U-based mono-EMFs characterized by single-crystal X-ray diffraction.

Table S8 The bond lengths (d , Å) and Wiberg bond indices (WBIs) between U and

the nearest C atom on the cage in $U@T_d-C_{27}B$ and $U@C_{2n}$.

species	<i>d</i>	WBI	species	<i>d</i>	WBI
$U@T_d-C_{27}B-1$	2.41	0.61	$U@C_{2v}(9)-C_{82}$	2.39	0.57
$U@T_d-C_{28}$	2.42	0.59	$U@C_2(8)-C_{84}$	2.44	0.57
$U@D_{3h}-C_{74}$	2.41	0.59	$U@C_s(15)-C_{84}$	2.47	0.52
$U@C_1(17418)-C_{76}$	2.47	0.51	$U@D_2(21)-C_{84}$	2.41	0.57
$U@C_1(228324)-C_{80}$	2.39	0.62	$U@C_1(11)-C_{86}$	2.41	0.58
$U@C_s(4)-C_{82}$	2.45	0.55	$U@C_1(12)-C_{86}$	2.48	0.51
$U@C_2(5)-C_{82}$	2.45	0.54	$U@C_s(15)-C_{86}$	2.41	0.58
$U@C_s(6)-C_{82}$	2.39	0.57			

Table S9 HOMO-LUMO gap energies (eV) of $U@T_d-C_{27}B^+$ as compared to isoelectronic $M@T_d-C_{28}$ at the PBE0/6-311G*~SDD level.

Species	HOMO-LUMO gap
$U@T_d-C_{27}B^+-1(U@T_d-C_{27}B^+-2)$	4.29(3.65)
$Th@T_d-C_{28}$	3.90
$Ti@T_d-C_{28}$	3.17
$Zr@T_d-C_{28}$	3.79
$Hf@T_d-C_{28}$	3.79

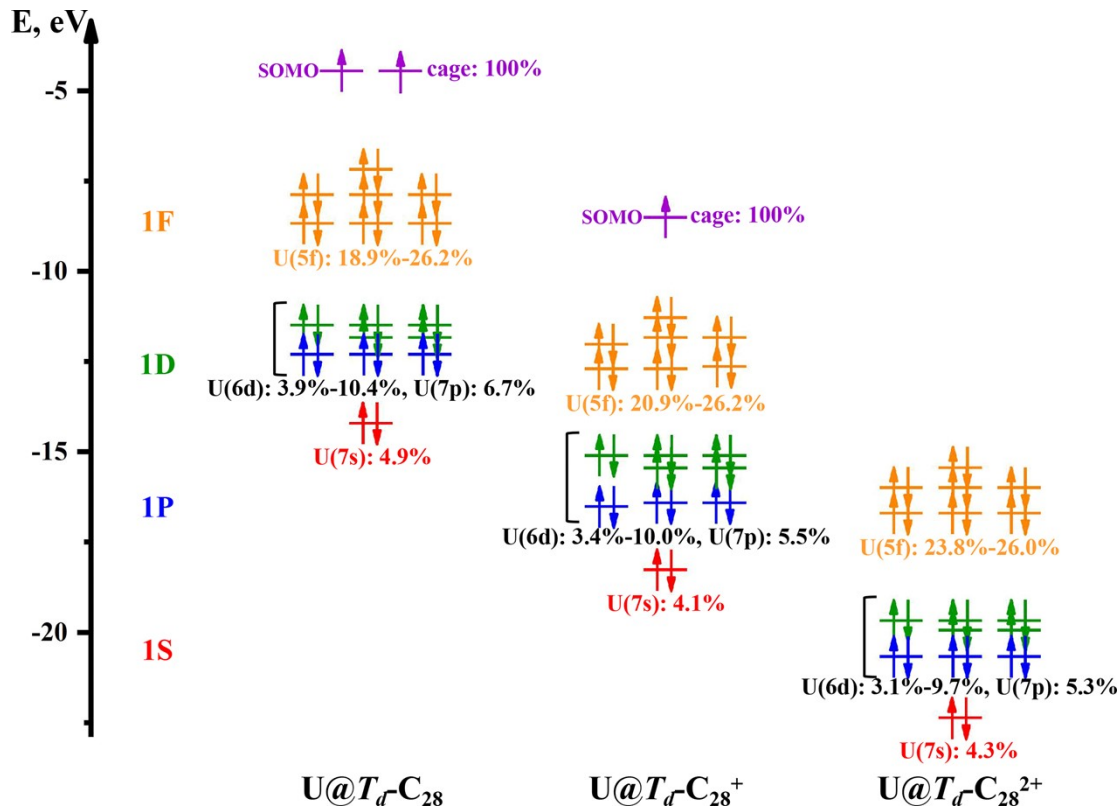


Fig. S13 Molecular orbital diagrams with the 16 orbitals involved in 32-electron closed-shell configuration of $U@T_d-C_{28}$, $U@T_d-C_{28}^+$ and $U@T_d-C_{28}^{2+}$. Spin up and

spin down orbitals are plotted as degenerated for simplicity. U orbital contributions to the hybrid orbitals are given in different colors.

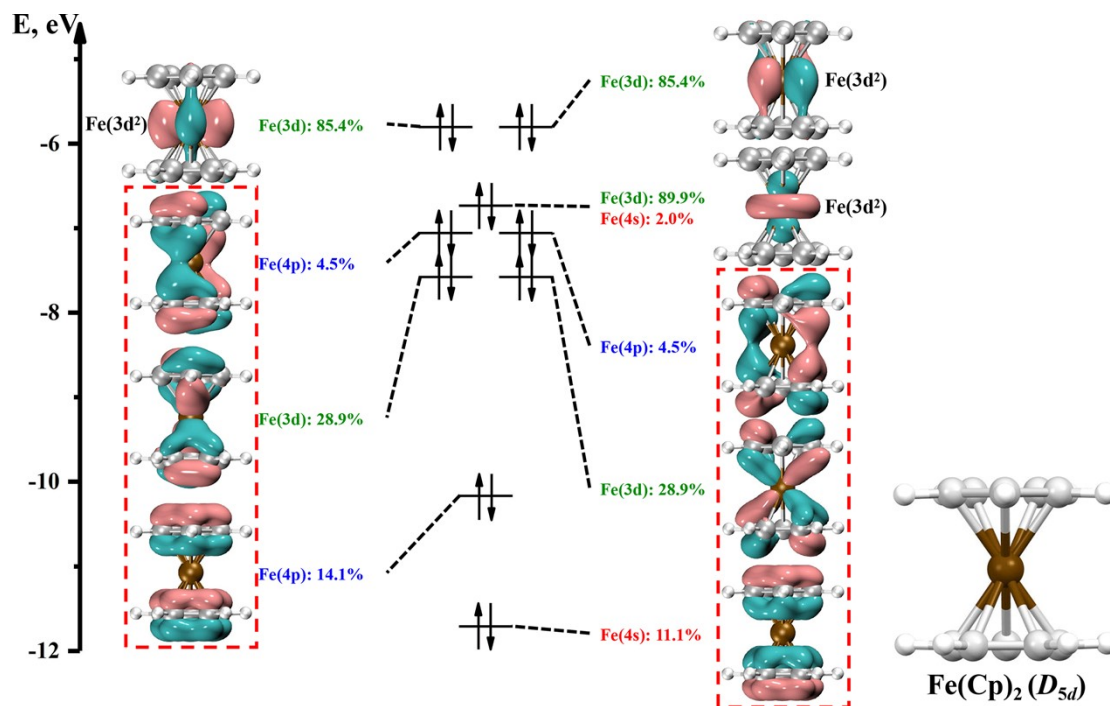


Fig. S14 Molecular orbital diagrams with the nine orbitals involved in 18-electron closed-shell configuration of ferrocene. Fe orbital contributions to the six Fe-(Cp)₂ hybrid orbitals (highlighted in red box) are given in different colors.

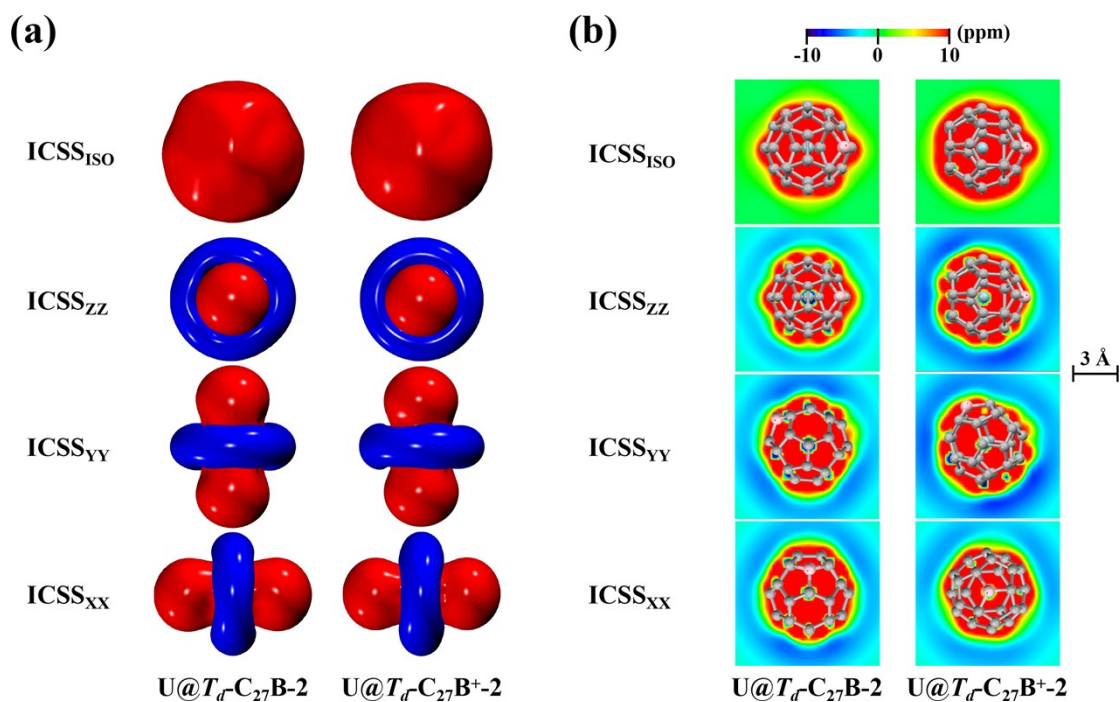


Fig. S15 (a) Three-dimensional isosurfaces (-2 to +2 ppm) and (b) Contour plot representations of ICSS of U@T_d-C₂₇B^{0/+}-2. Shielding and deshielding regions are in red and blue, respectively.

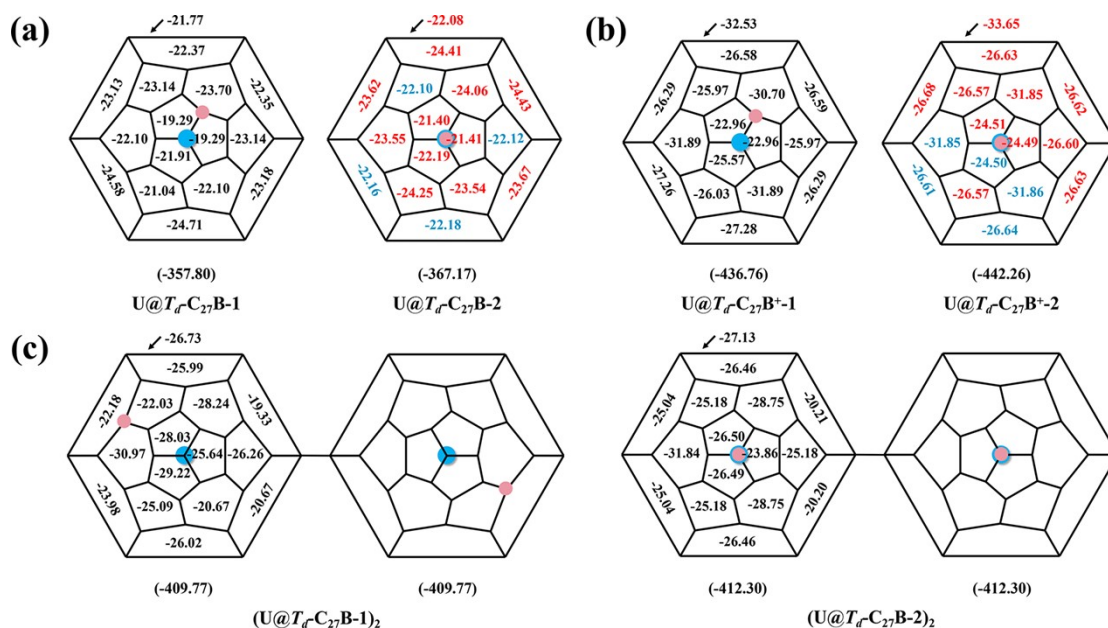


Fig. S16 NICS values (ppm) of (a) $U@T_d-C_{27}B$, (b) $U@T_d-C_{27}B^+$ and (c) $(U@T_d-C_{27}B)_2$ at all unequal rings and their Σ NICS (in parentheses). The U and B atoms are denoted by blue dots and pink dots in the Schlegel diagrams. For the $U@T_d-C_{27}B^{0/+}$, the increased and decreased local ring aromaticity compared to $U@T_d-C_{27}B^{0/+}-1$ are denoted by red and blue, respectively. Arrow represents the NICS value of the outer hexagonal ring.

Table S10 Relative energies (kcal/mol) of five $(U@T_d-C_{27}B)_2$ isomers with different spin multiplicities (M) at PBE0/6-311G*~SDD levels of theory.

Isomers	M	ΔE
$(U@T_d-C_{27}B-1)_2(C19-C19^*)$	1	0
	3	55.2
$(U@T_d-C_{27}B-1)_2(C15-C15^*)$	1	1.0
	3	50.2
$(U@T_d-C_{27}B-1)_2(C28-C28^*)$	1	4.9
	3	53.9
$(U@T_d-C_{27}B-1)-(U@T_d-C_{27}B-2)$	1	12.0
	3	59.0
$(U@T_d-C_{27}B-2)_2(C17-C17^*)$	1	23.7
	3	76.6

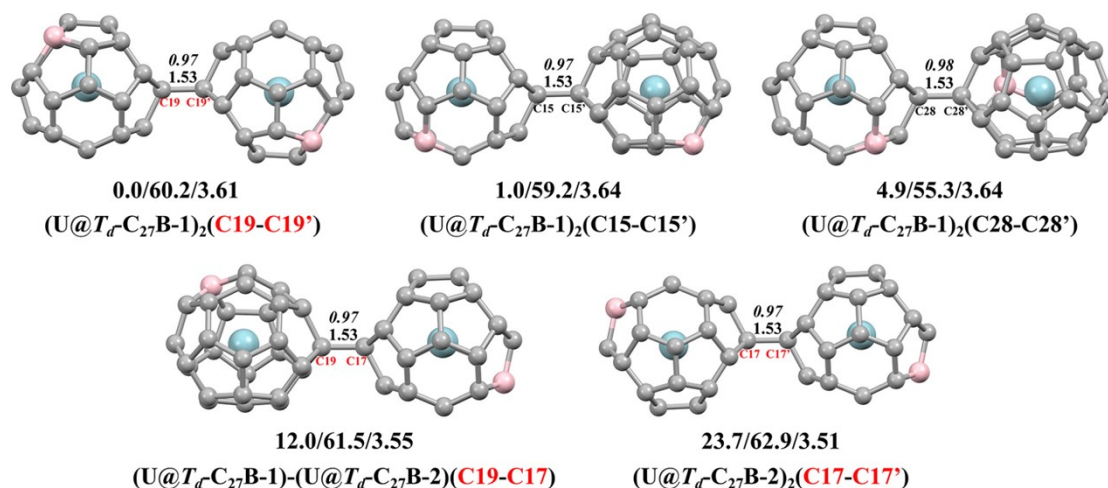
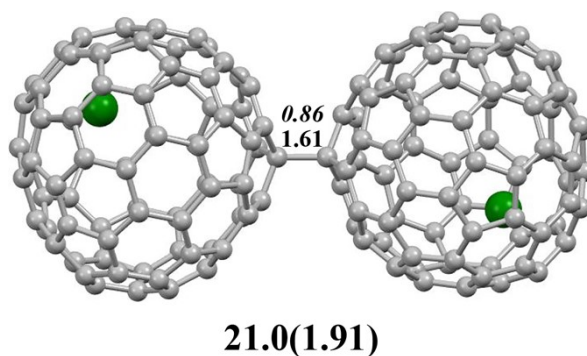


Fig. S17 Optimized structures of five dimer isomers with relative energies (kcal/mol)/dimerization energies (kcal/mol)/HOMO-LUMO gap energies(eV). The bond lengths are given in Å and WBIs are italic. The carbon sites in monomers with large spin density values in Fig. S8 are shown.



Y@C_s(6)-C₈₂ dimer

Fig. S18 Optimized structure of Y@C_s(6)-C₈₂ dimer with dimerization energy (kcal/mol) and HOMO-LUMO gap energy (eV, in parentheses) at the PBE0/6-311G*~SDD levels of theory. The bond length is given in Å and WBI is italic. C: gray; Y: green.

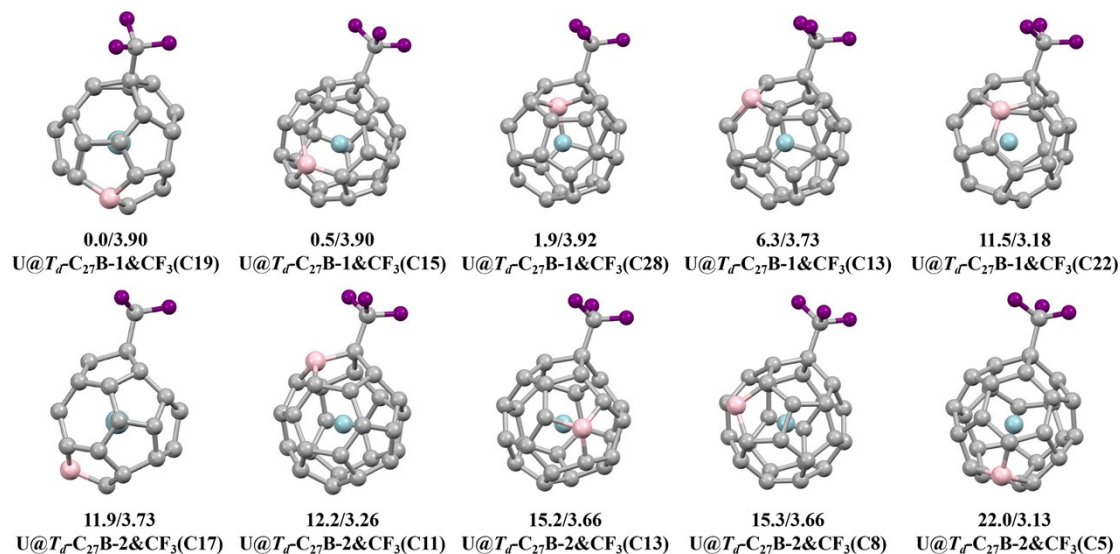


Fig. S19 Optimized structures with relative energies (kcal/mol)/HOMO-LUMO gap energies (eV) of possible $U@T_dC_{27}B&CF_3$ adduct isomers at different carbon sites in Fig. S9. C: gray; B: pink; F: purple; U: blue.

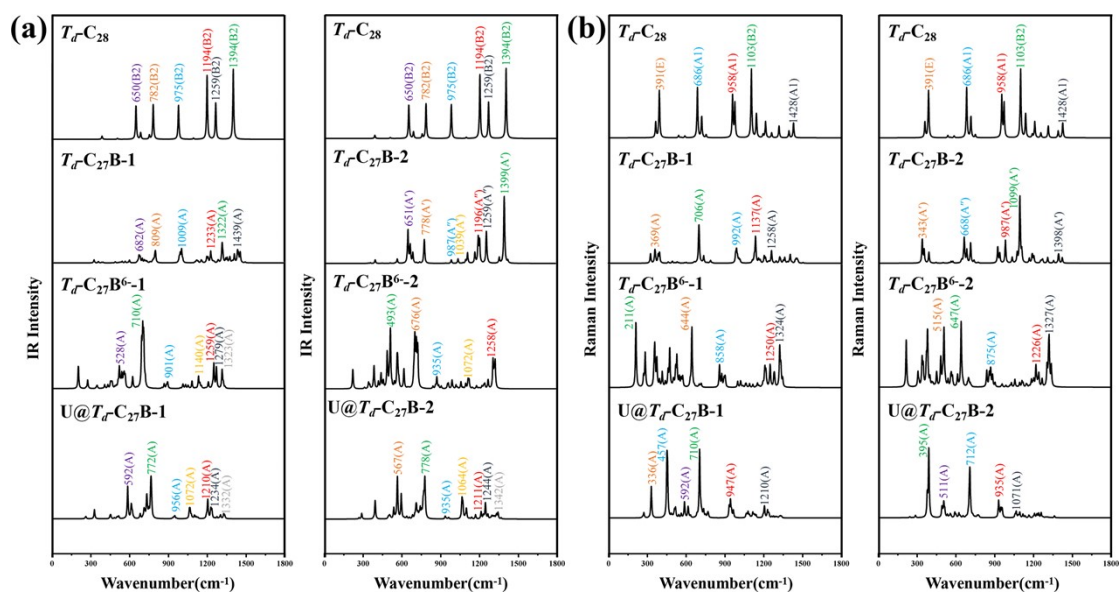


Fig. S20 (a) IR and (b) Raman spectra of two $U@T_dC_{27}B$ isomers and their corresponding empty parent cages.

Table S11 Relative energies (ΔE , kcal/mol) and HOMO(SOMO)-LUMO gaps (eV) of six classical and nonclassical (each contains a tetragon ring) C_{28} isomers at PBE0/6-311G*~SDD level of theory.

Isomer	ΔE	HOMO(SOMO)-LUMO gaps
T_dC_{28}	0.0	2.70
D_2C_{28}	33.6	1.85
$C_{28}(NC)-1$	25.3	2.03

C ₂₈ (NC)-2	46.9	2.46
C ₂₈ (NC)-3	43.6	2.04
C ₂₈ (NC)-4	79.4	2.18

Table S12 Relative energies (ΔE , kcal/mol) of twenty-nine classical and nonclassical U@C₂₇B isomers at PBE0/6-311G*~SDD level of theory.

Isomer	ΔE	Isomer	ΔE
U@T _d -C ₂₇ B-1	0.0	U@C ₂₇ B(NC)-15	58.7
U@C ₂₇ B(NC)-1	46.0	U@C ₂₇ B(NC)-16	59.7
U@C ₂₇ B(NC)-2	50.8	U@C ₂₇ B(NC)-17	59.7
U@C ₂₇ B(NC)-3	54.5	U@C ₂₇ B(NC)-18	60.1
U@C ₂₇ B(NC)-4	54.5	U@C ₂₇ B(NC)-19	60.2
U@C ₂₇ B(NC)-5	55.3	U@C ₂₇ B(NC)-20	64.3
U@C ₂₇ B(NC)-6	56.0	U@C ₂₇ B(NC)-21	64.5
U@C ₂₇ B(NC)-7	56.5	U@C ₂₇ B(NC)-22	65.6
U@C ₂₇ B(NC)-8	56.8	U@C ₂₇ B(NC)-23	69.1
U@C ₂₇ B(NC)-9	57.4	U@C ₂₇ B(NC)-24	70.2
U@C ₂₇ B(NC)-10	57.8	U@C ₂₇ B(NC)-25	71.1
U@C ₂₇ B(NC)-11	58.0	U@C ₂₇ B(NC)-26	72.5
U@C ₂₇ B(NC)-12	58.1	U@C ₂₇ B(NC)-27	72.8
U@C ₂₇ B(NC)-13	58.2	U@C ₂₇ B(NC)-28	73.7
U@C ₂₇ B(NC)-14	58.4		

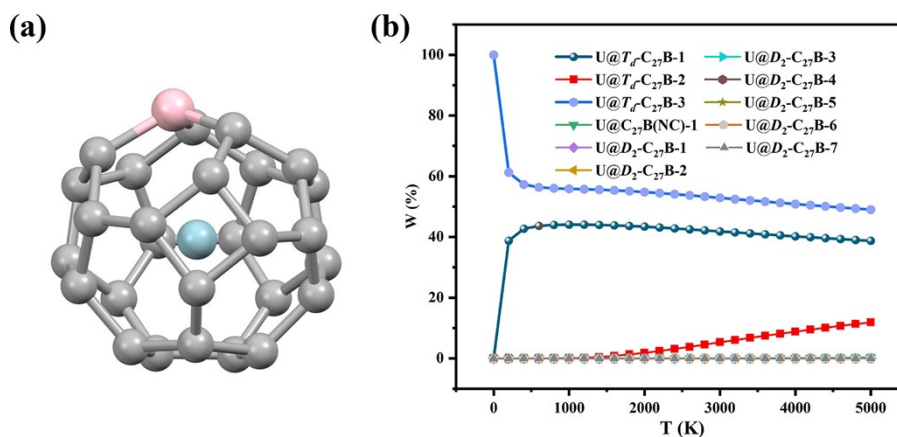


Fig. S21 (a) Optimized structure of U@C₂₇B(NC)-1 with a tetragon in the cage. (b) Relative concentrations of eleven classical and nonclassical U@C₂₇B isomers as a function of temperature at the PBE0/6-311G*~SDD level of theory.

Optimized Cartesian coordinates with the lowest vibrational frequency

U@T_d-C₂₇B-1 (272.0 cm⁻¹)

C -2.07616600 0.85706000 -1.03479600

C	-1.39681100	0.07821300	-2.05334800
C	-0.08437700	0.63727500	-2.34260900
C	0.03206900	1.86102000	-1.56456100
C	-1.18708600	1.99105700	-0.73537500
C	-2.41836400	-0.08093000	0.02327900
C	-1.91384000	-1.43877200	-0.36378400
C	-1.25692700	-1.31151400	-1.66644100
C	0.14767300	-1.67912000	-1.84060700
C	0.87773100	-0.44489800	-2.23298700
C	2.06326700	-0.25741500	-1.34348600
C	2.15442100	0.95347700	-0.55305700
C	1.20414200	2.04568300	-0.69858100
C	0.68237000	2.30890900	0.62892500
C	-0.76711000	2.22900800	0.63437200
C	-1.14139800	1.31393100	1.69895100
C	-2.02901100	0.17837500	1.39951800
C	-1.32257000	-1.00745100	1.84655200
C	-1.21017200	-1.99655000	0.79361900
C	0.19638600	-2.38661400	0.70383500
C	2.11351800	-1.37783900	-0.42260700
C	2.10787600	-0.89360000	0.94555600
C	2.18200300	0.55271100	0.88971700
C	1.24677900	1.40229000	1.60989500
C	0.10489800	0.78674100	2.29847400
C	0.00448600	-0.66449800	2.33658400
C	0.95163400	-1.52427700	1.65069500
B	0.91422200	-2.32498300	-0.66338400
U	-0.00177900	-0.01270400	-0.00358100

U@T_r-C₂₇B-2 (258.0 cm⁻¹)

C	-1.19072300	-1.26020000	-1.71820700
C	0.00507100	-2.03138100	-1.43281600
C	1.19095000	-1.24290500	-1.72768700
C	0.72564700	0.01459200	-2.32162500
C	-0.75460800	0.00262900	-2.32023500
C	-2.00244900	-1.27229900	-0.52484400
C	-1.24590000	-2.01603000	0.52292900
C	0.01972100	-2.47787100	-0.05318700
C	1.27643000	-1.99791700	0.52607700
C	2.02097600	-1.23217700	-0.54447700
C	2.55577700	0.02085300	0.00402300
C	2.00072000	1.26899600	-0.53523100
C	1.17042200	1.27510400	-1.71810400

C	-0.02783900	2.04204800	-1.41805700
C	-1.21120200	1.25376100	-1.70935100
C	-2.02262700	1.24424300	-0.51573400
C	-2.51206900	-0.02011800	0.05408100
C	-2.03993800	-0.02127300	1.43048500
C	-1.24210200	-1.19945000	1.72041600
C	0.01773900	-0.75595200	2.31057400
C	1.27573100	1.23918600	1.76604900
C	1.24390300	2.01437500	0.54074600
C	-0.02013100	2.47856700	-0.03520100
C	-1.27798100	1.99227500	0.53736900
C	-1.26109700	1.16755100	1.72882200
C	0.00573400	0.73956200	2.31586000
U	0.01289900	-0.00030800	0.00746200
C	1.29595400	-1.23155900	1.75677300
B	2.16733400	0.01213800	1.49535300

U@T_r-C₂₇B-3 (258.0 cm⁻¹)

C	-1.04403100	-1.48412900	1.61732600
C	-2.00781000	-0.42565700	1.40198900
C	-1.42088700	0.86326500	1.79419000
C	-0.10459200	0.55838300	2.36137300
C	0.13039300	-0.89679200	2.25928100
C	-0.92567700	-2.21629100	0.37712500
C	-1.79313300	-1.52493000	-0.61804300
C	-2.50035200	-0.43083000	0.03290000
B	-2.31158900	1.01428300	-0.48174000
C	-1.58221100	1.79548000	0.70195400
C	-0.38724100	2.43967100	0.14617200
C	0.93554900	2.12893900	0.67736100
C	1.06649000	1.23468700	1.80865200
C	2.02409800	0.21003800	1.43707300
C	1.44104200	-1.10071400	1.64210500
C	1.56141000	-1.81244700	0.39125500
C	0.39639700	-2.44523600	-0.22240200
C	0.31621700	-1.89761800	-1.56332300
C	-0.98371000	-1.29182700	-1.81101300
C	-0.73300600	0.06401200	-2.31904100
C	-0.32644000	2.10146500	-1.27779900
C	0.96775500	1.54363700	-1.60503200
C	1.78775100	1.59156000	-0.41667200
C	2.47248500	0.38163700	0.06733200
C	2.17564700	-0.88772300	-0.59611500

C	1.37305500	-0.93139700	-1.79575500
C	0.73063200	0.28338400	-2.30849900
C	-1.39978000	1.20735200	-1.70216500
U	-0.01589500	0.00631600	-0.00513800

INT (215.5 cm⁻¹)

C	1.12819700	1.83779600	-1.13872100
C	1.97738400	0.68255500	-1.34646900
C	2.50652800	0.26862100	-0.05886600
C	1.97197900	1.09543000	0.98579500
C	1.15609100	2.11960300	0.32378500
C	-0.11449400	1.56000300	-1.81630100
C	-0.07021900	0.13103100	-2.36230200
C	1.27070400	-0.43832500	-2.00390800
C	1.59340900	-1.60568100	-1.13222100
C	2.32787800	-1.11555700	0.02809500
C	1.46025600	-1.82311300	1.01580900
C	0.78359900	-0.99366600	1.99353500
C	1.18078600	0.43607900	2.06190100
C	-0.03475100	1.21781200	2.14078700
C	-0.08018700	2.20292500	1.06863500
C	-1.32525100	2.01805600	0.37354700
C	-1.37044500	1.77245400	-1.07968600
C	-2.10437600	0.55619600	-1.26505700
C	-1.35411300	-0.50806000	-1.96334700
C	-1.58023800	-1.72875900	-1.18665700
C	0.79541500	-2.44130600	-0.18723900
C	-1.36619300	-1.90183100	1.04077600
C	-0.73338600	-1.04292200	2.01548400
C	-1.20650800	0.37055100	2.12073900
C	-2.03764000	0.93379900	1.04548200
C	-2.54715000	0.08482400	0.01945900
C	-2.25280200	-1.30016500	0.05281100
B	-0.66230000	-2.56765700	-0.20857600
U	0.03765900	-0.01621500	-0.03730800

TS-1 (721.1i cm⁻¹)

C	1.97637200	-0.10754400	-1.43906800
C	1.56979300	-1.47557900	-1.27802800
C	1.63712100	-1.86448000	0.11577700
C	2.18193300	-0.74206700	0.84637500
C	2.42489500	0.36142300	-0.12864600
C	0.90226200	0.56100000	-2.17149100

C	-0.23828400	-0.41310000	-2.35174800
C	0.19525500	-1.69853500	-1.75325900
C	-0.53721800	-2.43628000	-0.76311500
C	0.35146500	-2.42329500	0.43634800
C	-0.47191100	-1.84926100	1.54048700
C	0.07408500	-0.71233500	2.28869700
C	1.41814900	-0.21397400	1.96082900
C	1.31716100	1.21880100	1.73476200
C	1.87544800	1.57713000	0.43961600
C	0.82919000	2.27623500	-0.28956600
C	0.38044000	1.79035800	-1.59626600
C	-1.05454000	1.63938800	-1.52866700
C	-1.48427800	0.27408100	-1.89562700
C	-2.42875700	-0.13856300	-0.87640500
C	-1.67410200	-1.61242200	0.79407200
C	-2.02629100	0.04531300	1.41890100
C	-0.86228200	0.43696500	2.19209000
C	-0.07517800	1.61135100	1.80908000
C	-0.36057400	2.34478400	0.59091400
C	-1.50279800	1.94132300	-0.19214000
C	-2.30738800	0.83300100	0.22437600
B	-2.91330500	-1.36828800	0.02467400
U	0.02072500	-0.00544400	-0.00970800

TS-2 (620.3i cm⁻¹)

C	-0.36099400	1.61832600	-1.77582400
C	1.03261900	1.75062000	-1.42601100
C	1.14829300	2.16673100	-0.04332600
C	-0.18783500	2.39781300	0.46644800
C	-1.14529600	2.06617200	-0.62240300
C	-0.53528300	0.28868600	-2.33977900
C	0.78150000	-0.44426700	-2.22486800
C	1.75374200	0.48953300	-1.61640600
C	2.50089100	0.25235900	-0.39349900
C	2.01126900	1.24423400	0.63381900
C	1.68560500	0.53376300	1.85307100
C	0.31204800	0.71408200	2.28561800
C	-0.59008900	1.67688200	1.66329600
C	-1.83883800	1.01615600	1.35069500
C	-2.16738300	1.20020800	-0.05905500
C	-2.36515800	-0.12727300	-0.61968100
C	-1.58161900	-0.55414500	-1.77770900
C	-0.95873000	-1.80669700	-1.42264500

C	0.49866100	-1.74627500	-1.59174100
C	1.10448600	-2.25672300	-0.39101800
C	2.93595200	-0.97315400	0.26552000
C	0.47341600	-1.71513000	1.84529100
C	-0.40083700	-0.61235900	2.29915400
C	-1.71697700	-0.39760900	1.67922300
C	-2.13685900	-1.11218400	0.47686200
C	-1.25146100	-2.13255500	-0.03992100
C	-0.00912800	-2.40967700	0.61344000
B	1.72194900	-1.33899200	1.04434200
U	-0.02784500	-0.00076300	0.00268500